



Trans. Nonferrous Met. Soc. China 34(2024) 3386-3399

Transactions of Nonferrous Metals Society of China

www.tnmsc.cn



Thermodynamic simulation of stepwise precipitation of NH₄VO₃ and NaHCO₃ from carbonating Na₃VO₄ solution

Fan-cheng MENG^{1,2}, Yong-chao WANG^{1,2}, Xin CHAI¹, Ya-hui LIU¹, Li-na WANG^{1,2}, De-sheng CHEN¹

- 1. National Engineering Research Center for Green Recycling of Strategic Metal Resources, Institute of Process Engineering, Chinese Academy of Sciences, Beijing 100190, China;
- 2. School of Chemical Engineering, University of Chinese Academy of Sciences, Beijing 101408, China

Received 5 April 2023; accepted 21 September 2023

Abstract: Thermodynamic simulation was conducted to design a new process of stepwise precipitating NH₄VO₃ and NaHCO₃ from regulating the CO₂ carbonation of Na₃VO₄ solution. Firstly, a new V(V) speciation model for the aqueous solution containing vanadate and carbonate is established by using the Bromley–Zemaitis activity coefficient model. Subsequently, thermodynamic equilibrium calculations are conducted to clarify the behavior of vanadium, carbon, sodium, and impurity species in atmospheric or high-pressure carbonation. To ensure the purity and recovery of vanadium products, Na₃VO₄ solution is initially carbonated to the pH of 9.3–9.4, followed by precipitating NH₄VO₃ by adding (NH₄)₂CO₃. After vanadium precipitation, the solution is deeply carbonated to the final pH of 7.3–7.5 to precipitate NaHCO₃, and the remaining solution is recycled to dissolve Na₃VO₄ crystals. Finally, verification experiments demonstrate that 99.1% of vanadium and 91.4% of sodium in the solution are recovered in the form of NH₄VO₃ and NaHCO₃, respectively.

Key words: thermodynamics; sodium orthovanadate; speciation model; carbonation; vanadium precipitation; sodium bicarbonate

1 Introduction

Sodium orthovanadate (Na₃VO₄) crystals are usually crystallized from highly concentrated alkali solutions containing vanadium [1]. These crystals exhibit high purity and can be used as feasible raw materials for the production of V₂O₅ [2], which is the leading vanadium product widely used in metallurgy and chemical engineering [3,4]. Several newly developed processes, such as the direct reduction–sodium smelting and comprehensive utilization process of vanadium-bearing titanomagnetite [5,6], low-pressure NaOH oxidative leaching process of vanadium slag [7,8], and alkaline leaching–crystallization process of V–Cr

bearing reducing slag [9], all produced the intermediate product of Na₃VO₄ crystals. The Na/V molar ratio of sodium orthovanadate solution typically exceeds 3.0, which is significantly higher than the ratio of 1.0-1.5 observed in industrial alkaline vanadium-containing solutions obtained from vanadium slag [10,11]. However, if subjected to the traditional V₂O₅ production process, i.e., acidification via sulfuric acid, vanadium precipitation using ammonium salts, and subsequent calcination [12,13], the sodium orthovanadate solution will consume more sulfuric acid, thereby resulting in the generation of excessive useless Na₂SO₄ and the elevated treatment cost associated with ammonia-nitrogen wastewater [14]. Besides, V₂O₅ can also be prepared by the calcination of NH_4VO_3 precipitated from low alkaline solution. To successfully prepare V_2O_5 using sodium orthovanadate, a green and efficient process must be carefully designed, considering the recovery of vanadium and sodium, as well as the recycling of ammonium medium.

CO₂ carbonation is a promising approach that can reduce the pH of alkaline vanadium-containing solution, recover sodium salts, and utilize the discharged CO₂ gas [14]. ZHOU et al [15] used CO₂ to carbonate the NaOH-concentrated vanadiumcontaining solution, but the precipitation of NaHCO₃ before vanadium precipitation caused high vanadium loss. Besides, the use of NH₄Cl to precipitate vanadium introduced chloride anion impurity into the system, and the evaporation for NaHCO₃ recovery and ammonia distillation required high energy consumption in the process. LONG et al [16] carbonated the highly alkaline vanadium-containing solution with CO₂ to separate vanadium and silicon, but how to determine the end point of carbonation was not discussed. In the above processes, the behavior of vanadium, carbon, sodium, and impurity species remained unclear, which is a key issue to design a new process based on the carbonation of Na₃VO₄ solution.

Thermodynamic simulation is a powerful tool to assist the process design and optimization [17,18], especially when dealing with the complex gas-liquid-solid reactions and equilibria involved in the carbonation of Na₃VO₄ solution and vanadium precipitation. The speciation model of V(V) in aqueous solution is the basis of thermodynamic calculations. Over the past forty years, several speciation models of V(V) have been established based on ⁵¹V NMR and potentiometric titration [19-21]. However, these studies were carried out with different ionic salts or at high ionic strengths, and no attempt was made to reconcile NMR results with older data. As a result, large discrepancies of equilibrium constants emerged [22], leading to controversies when directly using these data in some studies [23,24], and even in the software of Visual MinTEQ [25] and Hydra-Medusa [26]. The latest studies by MCCANN et al [27] and LARSON [22] have determined the equilibrium constants of V(V) species independent of ionic strength, and employed the extended Debye-Hückel equation to estimate the activity coefficient. However, due to

the deficiency of the activity model, the above speciation models are limited to solutions with the vanadium concentration of lower than 0.1 mol/L. In addition, previous studies only considered the V(V)–H₂O system, neglecting the carbonate complexes of vanadate. Therefore, establishment of a new V(V) speciation model is necessary for conducting thermodynamic calculations.

In this study, thermodynamic simulation was conducted to assist in designing a new process to stepwise precipitate NH₄VO₃ and NaHCO₃ from regulating the carbonation of Na₃VO₄ solution. Based on the establishment of a new V(V) speciation model for the aqueous solution containing vanadate and carbonate, thermodynamic equilibria of the involved reactions were calculated to determine the starting and final pH of solutions in different steps. After that, the new process was proposed and verified by experiments.

2 Thermodynamic simulation and experiment

2.1 Details of thermodynamic simulation

2.1.1 Establishment of new V(V) speciation model

Through critical comparison and selection, various vanadium species can be found in V(V)– H_2O system, including VO_4^{3-} , HVO_4^{2-} , $H_2VO_4^{-}$, $V_2O_7^{4-}$, $HV_2O_7^{3-}$, $H_2V_2O_7^{2-}$, $HV_3O_{10}^{4-}$, $V_4O_{13}^{4-}$, $V_4O_{15}^{4-}$, $V_5O_{15}^{5-}$, $V_{10}O_{28}^{6-}$, $HV_{10}O_{28}^{5-}$, $H_2V_{10}O_{28}^{4-}$, and VO_2^{+} . The thermodynamic data and formation constants of vanadium species are listed in Table 1. The involved equilibrium reaction is expressed as follows:

$$pH_2VO_4^- + qH^+ = H_zV_pO_m^{n-} + (q/2 + p - z/2)H_2O$$
 (1)

When it comes to the aqueous solution containing vanadate and carbonate, the carbonate complexes of vanadate, including HVO₃CO₃²⁻ and VO₂(CO₃)₂³⁻, should also be considered, and the equilibrium reactions are written as follows [30]:

$$H_2VO_4^- + HCO_3^- = HVO_3CO_3^{2-} + H_2O$$
 (2)

$$H_2VO_4^- + 2HCO_3^- = VO_2(CO_3)_2^{3-} + 2H_2O$$
 (3)

The mathematical relationships between vanadium species in V(V)- H_2O system are described as follows:

$$\{H_z V_p O_m^{n-}\} = K \cdot \{H_2 V O_4^-\}^p \cdot \{H^+\}^q$$
 (4)

$$\{\mathbf{H}_z \mathbf{V}_p \mathbf{O}_m^{n-}\} = \gamma_i [\mathbf{H}_z \mathbf{V}_p \mathbf{O}_m^{n-}] \tag{5}$$

$$\Sigma[H_z V_p O_m^{n-}] = [V]_{\text{total}}$$
 (6)

Table 1 Thermodynamic data of V(V) species in aqueous solution containing vanadate and carbonate at 298.15 K

		\ / I						
Species	$\Delta G_{\rm f}/({\rm kJ\cdot mol^{-1}})$	$\Delta H_{\rm f}/({\rm kJ \cdot mol^{-1}})$	$S/(J \cdot \text{mol}^{-1} \cdot \text{K}^{-1})$	$C_{p,m}/(\mathbf{J}\cdot\mathbf{mol}^{-1}\cdot\mathbf{K}^{-1})$	q^{a}	p^{a}	lg K ^a	Ref.
Na_3VO_4	-1637.8	-1758.1	190	164.9				[28]
$NaVO_3$	-1066.9	-1148.6	113.9	97.6				[28]
$\mathrm{H}_2\mathrm{VO}_4^-$	-1022.5	-1174.2	126	149.9				[22,29]
VO_4^{3-}	-899.5	-1132.7	-147.34	159.1	-2	1	-21.54	[22,29]
HVO_4^{2-}	-972.5	-1167.4	-19.0	365.4	-1	1	-8.76	[22,29]
VO_2^+	-587.0	-649.8	-42.3	-57.4	2	1	6.85	[22,29]
$V_2O_7^{4-}$	-1701.7	-2096.3	-287		-2	2	-18.59	[22]
$HV_2O_7^{3-}$	-1766.1	-2096.9	-71		-1	2	-7.31	[22]
$H_{2}V_{2}O_{7}^{2-} \\$	-1820.9	-2092.9	124		0	2	2.29	[22]
$HV_3O_{10}^{4-}$	-2558.3	-2968.9	60.9		-1	3	-6.10	[22,27]
$V_4O_{13}^{6-}$	-3286.6	-3852.3	-57.7		-2	4	-16.10	[22,27]
$V_4O_{12}^{4-}$	-3185	-3648	52		0	4	7.66	[22]
$V_5O_{15}^{5-}$	-3969.4	-4548.9	65.0		0	5	7.50	[22,27]
$V_{10}O_{28}^{6-}$	-7653				4	10	48.00	[22,27]
$HV_{10}O_{28}^{5-}$	-7687	-8650	266		5	10	53.98	[22]
$\mathrm{H_{2}V_{10}O_{28}^{4-}}$	-7711				6	10	58.18	[22]
$HVO_3CO_3^{2-}$	-1388.5						11.42	[22,30]
$VO_2(CO_3)_2^{3-}$	-1743.3						20.83	[22,30]

^a Stoichiometric coefficients and formation constants for the equilibrium reaction of Eq. (1)

where $\{\}$ and [] represent the activity and concentration (as molarity) in the solution; K represents the formation constants in Table 1; γ represents the activity coefficient.

Other species and corresponding equilibrium equations used in thermodynamic calculations can be found in Table S1 in the Supplementary materials. Since the new process involves high ionic strength solutions (μ >3.0 mol/L), it is imperative to incorporate a more accurate correction of activity coefficient in calculations, which was usually omitted in previous studies due to its complexity [31,32]. To address this issue, activity models specifically designed for high ionic strength solutions have been developed, which mainly include the NRTL model [33], the Bromley-Zemaitis model [34,35], and the mixed-solvent electrolyte model [36]. Considering the availability of model parameters and its successful applications electrolytes with the concentration 0-30 mol/kg at $0-200 \,^{\circ}\text{C}$ [37], the Bromley-Zemaitis activity model was used in calculations by the Stream Analyzer module of OLI Studio 11 software, which is described by Eq. (7) [34,35]:

$$\lg \gamma_{i} = -\frac{AZ_{i}^{2}\sqrt{I}}{1+\sqrt{I}} + \sum_{j} \{ [(0.06+0.6B)|Z_{i}Z_{j}|] / \left(1 + \frac{1.5}{|Z_{i}Z_{j}|}I\right)^{2} + B_{ij} + C_{ij}I + D_{ij}I^{2} \} \cdot \left(\frac{|Z_{i}| + |Z_{j}|}{2}\right)^{2} c_{i}$$

$$\left(\frac{|Z_{i}| + |Z_{j}|}{2}\right)^{2} c_{i} \tag{7}$$

where γ_i is the activity coefficient of anion i in electrolyte solution; j is the cation in solution; k is the Debye–Hückel parameter; k is the ionic strength of the solution (as molarity); k is the molarity-based concentration of anions; k, k, and k are temperature-dependent empirical coefficients; k and k are the anion and cation charges, respectively.

2.1.2 Calculation of ΔG , ΔH , and phase diagram

Reaction module in FactSage 8.1 was used to calculate the free energy change (ΔG) and enthalpy change (ΔH) of carbonation reactions at 25–100 °C and CO₂ pressure of 101.325–1013.25 kPa. The phase diagram of the Na₃VO₄–CO₂–H₂O system was established by the phase diagram module in

FactSage 8.1. The pure substances and aqueous species in Table 1 were used in priority in these calculations.

2.1.3 Thermodynamic equilibrium calculation of involved reactions

The practical sodium orthovanadate crystals obtained from industrial sources generally contain silicon and aluminum impurities, and the representative sodium orthovanadate solution containing 1 mol/kg Na₃VO₄, 0.1 mol/kg Na₂SiO₃, and 0.01 mol/kg NaAlO₂ was used in calculations. It is worth noting that the above-mentioned sodium orthovanadate crystals contain negligible amounts of phosphorus, so phosphorus was not considered in this study.

Thermodynamic equilibria of the involved reactions of carbonation, precipitation, and solution recycling were calculated by the Stream Analyzer module in OLI Studio 11 software using the Bromley–Zemaitis activity model. The established new V(V) speciation model was used in the calculations, so the species in Table 1 were used in priority, and the other species were from the OLI PUB database. Unless otherwise specified, all equilibrium calculations were based on 1 kg of H₂O.

2.2 Experimental procedures

The composition of the practical sodium orthovanadate containing impurities was 37.5% Na, 25.8% V, 1.4% Si, and 0.1% Al. The sodium orthovanadate crystals without silicon and aluminum impurities, in the phase of Na₃VO₄-(NaOH)_{0-0.25}·12H₂O, were obtained from our recent study [14].

CO₂ gas was injected into 1.2 mol/L Na₃VO₄ solution in a nickel autoclave with the mechanical stirring to carry out the atmospheric carbonation at 25 °C. Subsequently, (NH₄)₂CO₃ was added into the carbonated solution with the NH₄⁺/V molar ratio of 1:1 to precipitate vanadium at 25 °C. Finally, the solution after vanadium precipitation was carbonated with 1 MPa CO₂ at 25 °C to recover solid NaHCO₃, and the remaining solution was recycled to dissolve Na₃VO₄ crystals. The pH of solutions in these steps was monitored using a composite pH probe (REX PHS-3C, INESA). The solutions and solids were sampled and analyzed. The concentrations of HCO₃⁻ and CO₄²⁻ were determined by the titration method [38], indicating

the titration end point with the pH meter and subtracting the blank value of vanadate at the corresponding pH value. The concentrations of vanadium and sodium were determined by inductively coupled plasma optical emission spectrometry (ICP-OES, Optima 5300DV, PerkinElmer). Moreover, the phase of solids was identified using X-ray diffraction (XRD, Empyrean, PANalytical) with Cu K $_{\alpha}$ radiation operating at 40 kV and 40 mA from 5° to 90°.

3 Results and discussion

3.1 Vanadium distribution with new V(V) speciation model

A new speciation model of V(V) was established in Section 2.1.1, serving as a crucial basis for thermodynamic calculations. The calculated vanadium molar distribution of V(V) species under different pH at [V]=1.0 mol/L at 25 °C is shown in Fig. 1.

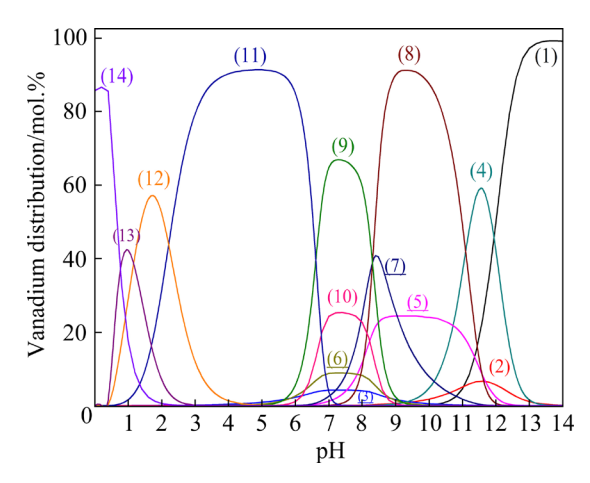


Fig. 1 Vanadium distribution of vanadium species in V(V)-H₂O system at 25 °C at various pH with [V]= 1.0 mol/L: (1) VO₄³⁻; (2) HVO₄²⁻; (3) H₂VO₄⁻ (×100); (4) V₂O₇⁴⁻; (5) HV₂O₇³⁻ (×100); (6) H₂V₂O₇²⁻ (×100); (7) HV₃O₁₀⁴⁻ (×100); (8) V₄O₁₃⁶⁻; (9) V₄O₁₂⁴⁻; (10) V₅O₁₅⁵⁻; (11) V₁₀O₂₈⁶⁻; (12) HV₁₀O₂₈⁵⁻; (13) H₂V₁₀O₄₈⁴⁻; (14) VO₂⁴⁻

As depicted in Fig. 1, almost 100% of vanadium in solution exists in the form of VO_4^{3-} within the pH range of 13–14. With the decrease of pH, the vanadium distribution of VO_4^{3-} gradually reduces, transforming into the poly-vanadate anions of $V_4O_{13}^{6-}$, $V_2O_7^{4-}$ and HVO_4^{2-} within the pH range of 9–13 and $V_4O_{12}^{4-}$, $V_5O_{15}^{5-}$ and $V_4O_{13}^{6-}$ within the pH range of 7–9. To be specific, the vanadium distributions of $V_2O_7^{4-}$, $V_4O_{13}^{6-}$, and $V_4O_{12}^{4-}$ at pH

 $Na_3VO_4+2CO_2+H_2O=NaVO_3+2NaHCO_3$ (9)

values of 11.6, 9.3, and 7.3 reach 59.0, 91.2, and 66.8 mol.%, respectively. $V_4O_{13}^{6-}$ is the linear tetrameric species, while $V_4O_{12}^{4-}$ is the more stable cyclic form that appears under near-acidic conditions [27]. The concentrations of $HV_3O_{10}^{4-}$, $HV_2O_7^{3-}$, $H_2V_2O_7^{2-}$, and $H_2VO_4^{-}$ are very low, and they are magnified by 100 times in Fig. 1 for clarity. $V_{10}O_{28}^{6-}$, $HV_{10}O_{28}^{5-}$, and $H_2V_{10}O_{28}^{4-}$ become the main species within the pH range of 1.5–6.0, and they transform into six-coordinated cationic species (VO_2^+) at pH<1.

To illustrate the effect of vanadium activity on the distribution of vanadium species, Fig. 2 presents the $\lg a$ -pH diagram calculated by using the established V(V) speciation model (a is the activity). It is indicated that the formation of poly-vanadate anions is strongly dependent on vanadium activity, occurring only when $\{V\}>10^{-3}\,\text{mol/L}$. Within the pH range of 7–10 at $\{V\}>0.1\,\text{mol/L}$, the main species are $V_4O_{13}^{6-}$ and $V_4O_{12}^{4-}$.

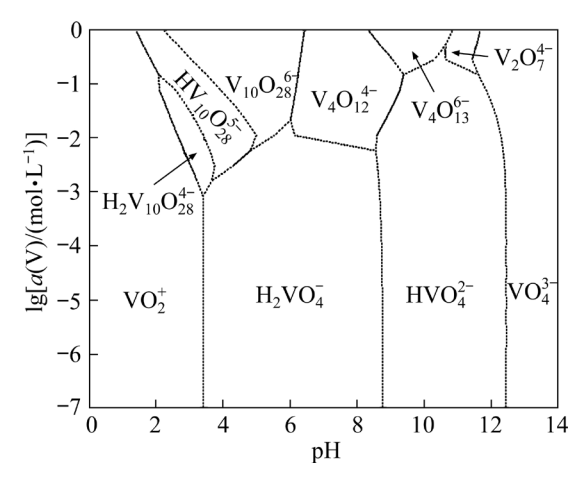


Fig. 2 lg a-pH diagram of V(V)-H₂O system at 25 °C and 101.325 kPa (a is the activity)

3.2 Phase diagrams, ΔG and ΔH of carbonation reactions

According to the phase diagram of the Na₃VO₄–CO₂–H₂O system presented in Fig. 3, no additional compounds except Na₃VO₄, NaVO₃, Na₂CO₃, and NaHCO₃ are observed. With the increase of CO₂ amount, the dotted line representing a Na₃VO₄ molality of 1 mol/kg in Fig. 3 passes through the "NaHCO₃+aq." region, indicating the feasibility of separating NaHCO₃ from vanadium-containing solution.

As discussed above, the carbonation reactions may be written as follows:

$$Na_3VO_4+CO_2=NaVO_3+Na_2CO_3$$
 (8)

Figure 4 indicates that ΔG of these reactions is negative at the investigated temperatures, and the formation of NaVO₃ and NaHCO₃ is more favorable. Furthermore, increasing CO₂ pressure from 101.325

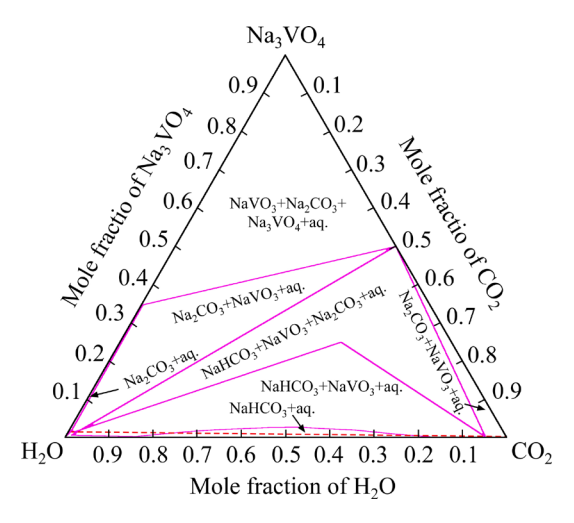


Fig. 3 Phase diagram of Na_3VO_4 – H_2O – CO_2 at 25 °C and 101.325 kPa

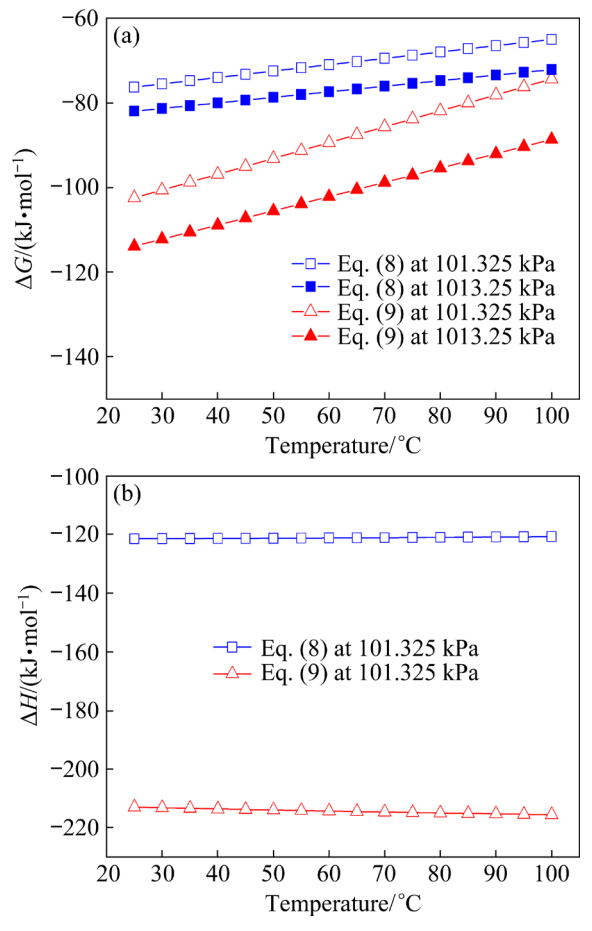


Fig. 4 Gibbs free energy change (a) and enthalpy change (b) of carbonation reactions under different temperatures and CO₂ pressures

to 1013.25 kPa is beneficial to the reactions. Additionally, both reactions are exothermic, with ΔH remaining almost constant from 25 to 100 °C.

Using the established V(V) speciation model, thermodynamic equilibrium calculations on both sides of Eqs. (8) and (9) were calculated, as shown in Table 2. The results demonstrate that the type and amount of the species on the left and right sides of Eqs. (8) and (9) are the same, and the pH of these two solutions are 9.32 and 7.51, respectively. These findings indicate that the established V(V) speciation model for the aqueous solution containing vanadate and carbonate aligns well with the carbonation reactions described in Eqs. (8) and (9).

3.3 Thermodynamic equilibrium calculations of involved reactions

3.3.1 Atmospheric carbonation

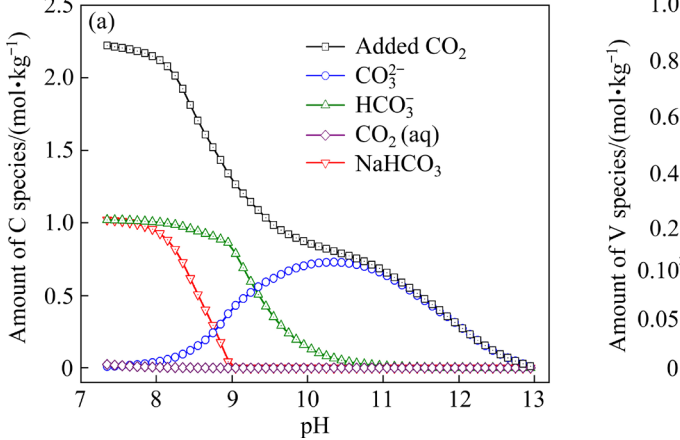
To simulate the carbonation of the Na₃VO₄ solution containing silicon and aluminum impurities, the representative Na₃VO₄ solution was used for the calculations. Figure 5(a) shows the calculated

equilibrium amount of added CO₂ and formed carbon species in atmospheric carbonation. With the addition of CO₂, the amount of CO₃²⁻ initially increases, reaching its maximum at pH= 10.3, and then reduces to almost zero at the end of carbonation (pH=7.35). The end point of carbonation is that Na₃VO₄ has been completely transformed into NaHCO₃ and NaVO₃, and a certain amount of CO₂ gas is also dissolved in the solution, reaching a gas-liquid or gas-liquid-solid equilibrium. The amount of HCO₃ increases with the decrease of pH, and solid NaHCO₃ starts to precipitate at pH=8.95 and finally reaches 1.02 mol at pH=7.35.

As indicated by the calculation results in Fig. S1 in the Supplementary materials, when pure Na₃VO₄ solution of 1 mol/kg is used, 2.018 mol CO₂ is consumed at the end of atmospheric carbonation, which is slightly more than the stoichiometry value of 2.0 mol when forming NaHCO₃ in Eq. (9). The excessive 0.018 mol CO₂ is mainly attributed to the physical dissolution of CO₂ in the solution.

Table 2 Thermodynamic equilibria of carbonating Na₃VO₄ solution with CO₂ and mixing NaVO₃ solution with Na₂CO₃ or NaHCO₃ at 25 °C and 101.325 kPa

No.	T // 1	рН —	Main species output/mol					
	Input/mol		CO_3^{2-}	HCO_3^-	$V_4O_{13}^{6-}$	$V_4O_{12}^{4-}$		
A1	1Na ₃ VO ₄ +1CO ₂ +55.5082H ₂ O	9.32	0.497	0.491	0.241	0.001		
A2	$1 NaVO_3 + 1 Na_2 CO_3 + 55.5082 H_2 O$	9.32	0.497	0.491	0.241	0.001		
A3	1Na ₃ VO ₄ +2CO ₂ +55.5082H ₂ O	7.51	1.020	0.013	0.002	0.171		
A4	1NaVO ₃ +2NaHCO ₃ +54.5082H ₂ O	7.51	1.020	0.013	0.002	0.171		



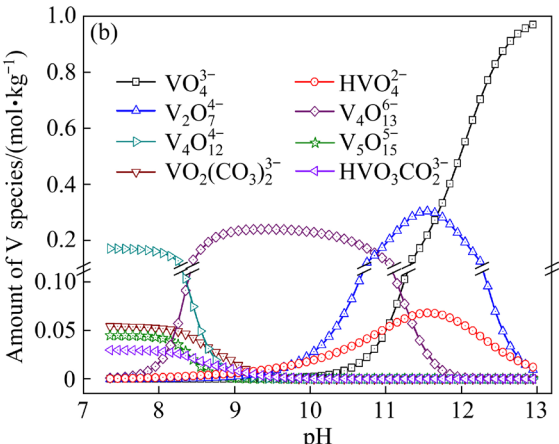


Fig. 5 Equilibrium amount of carbon species (a) and vanadium species (b) versus pH in carbonating representative Na₃VO₄ solution at 25 °C and 101.325 kPa

Figure 5(b) illustrates that the amount of VO_4^{3-} decreases rapidly, reaching 0.01 mol at pH=10.5. VO_4^{3-} transforms into $V_2O_7^{4-}$, HVO_4^{2-} and $V_4O_{13}^{6-}$ anions successively, and $V_4O_{13}^{6-}$ is the dominant species of vanadium within the pH range of 9–10. $VO_2(CO_3)_2^{3-}$ and $HVO_3CO_3^{2-}$ appear at pH=9.8, and their amounts are only 0.030 and 0.054 mol at pH=7.35, respectively, indicating that more than 90% of vanadium has been transformed into $V_4O_{12}^{4-}$ and $V_5O_{15}^{5-}$ by carbonation.

To verify the accuracy of thermodynamic calculations, the compositions of $CO_3^{2^-}$ and HCO_3^- in carbonating the Na_3VO_4 solution ([V]=60 g/L, Na/V molar ratio of 3.24) were experimentally detected and compared with the calculation results. Figure 6 indicates that the deviation between the calculated and experimental results is relatively small. The formed $VO_2(CO_3)_2^{3^-}$ and $HVO_3CO_3^{2^-}$ may decompose and release HCO_3^- in analysis, leading to a slightly larger discrepancy at pH<8.0.

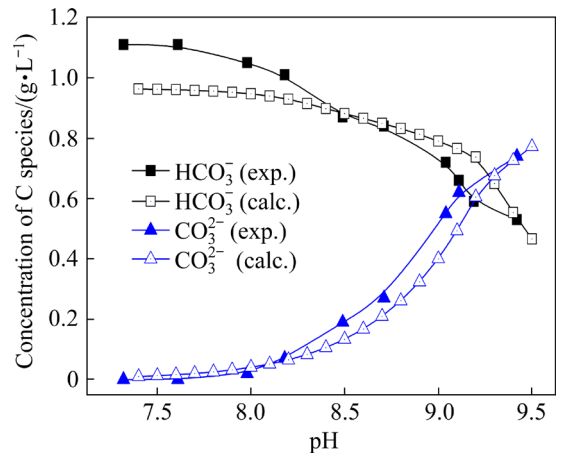


Fig. 6 Experimental and calculated CO₃²⁻ and HCO₃⁻ concentration in carbonating Na₃VO₄ solution at 25 °C and 101.325 kPa

The behavior of silicon and aluminum species in carbonation is the basis for determining the appropriate strategy for impurity Figure 7(a) illustrates a significant decrease in the amount of soluble species NaHSiO₃ and H₃SiO₄ at pH=9.6, which corresponds to the precipitation of solid SiO₂. Solid SiO₂ accounts for 98% of the total silicon at pH<8.5, suggesting that most of the silicon can be effectively removed under this condition. As shown in Fig. 7(b), with the decrease of pH, Al(OH)₄ gradually transforms into insoluble Al(OH)₃ at pH<11.8. The presence of CO_3^{2-} and a low $K_{\rm sp}$ value of $10^{-33.3}$ for NaAl(OH)₂CO₃

(dawsonite) [39] promote subsequent transformation of Al(OH)₃ into dawsonite. Remarkably, more than 99% of aluminum exists in the form of dawsonite at pH<11.4, indicating a high removal efficiency of aluminum by carbonation.

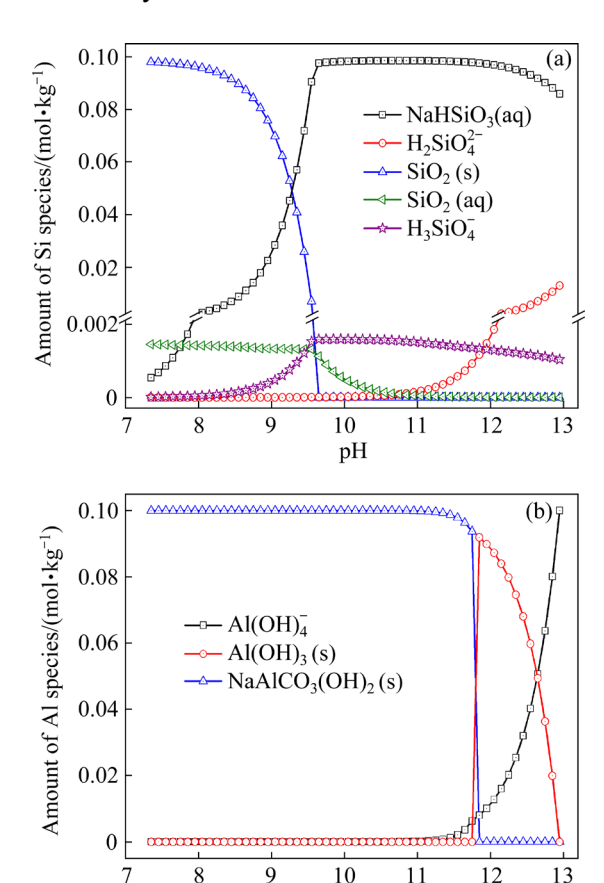


Fig. 7 Equilibrium amount of silicon species (a) and aluminum species (b) versus pH in carbonating representative Na₃VO₄ solution at 25 °C and 101.325 kPa

рН

assess the progress of atmospheric carbonation, several important parameters need to be considered, namely, pH₀ (initial pH), pH_C (pH value that CO₃²⁻ reaches the maximum), pH_H (pH value that solid NaHCO₃ starts to precipitate), pH_F (final pH value of carbonation), as well as the amount of NaHCO₃ precipitation and CO₂ consumption. The effect of carbonation temperature on these parameters is depicted in Fig. 8(a). With the increase of temperature, there is a decrease in pH₀, pH_C, and pH_H but a slight increase in pH_F. Specifically, the calculated pH_F of atmospheric carbonation at 25 °C is 7.33, whereas it increases to 7.77 at 55 °C due to the increased amount of soluble NaHCO3. Moreover, the complete elimination of solid NaHCO3 is observed at 55 °C,

indicating that higher carbonation temperatures are unfavorable for NaHCO₃ recovery.

Figure 8(b) demonstrates that an increase in Na₃VO₄ concentration leads to higher pH₀, pH_C, and pH_H and lower pH_F (from 7.30 at 0.4 mol/kg to 7.19 at 2.0 mol/kg). Solid NaHCO₃ starts to precipitate when the Na₃VO₄ concentration reaches 0.6 mol/kg. Subsequently, solid NaHCO₃ precipitation and CO₂ consumption exhibit nearly linear growth with increasing Na₃VO₄ concentration. To ensure efficient recovery of solid NaHCO₃, Na₃VO₄ concentration should be higher than 0.8 mol/kg.

3.3.2 High-pressure carbonation

High pressure of CO₂ is known to be beneficial to carbonation reactions, so the thermodynamic equilibrium of high-pressure carbonation was calculated. The total pressure in this system is slightly higher but very close to the partial pressure of CO₂. Figure 9(a) indicates that the increase of total pressure leads to a decrease in the final pH of

carbonation (from pH=7.02 at 0.2 MPa to pH=6.24 at 1.5 MPa) and an increase in the amount of NaHCO₃ precipitate and CO₂ consumption. As shown in Fig. 9(b), an increase of temperature at the total pressure of 1 MPa results in a noticeable decrease in CO₂ consumption and NaHCO₃ precipitate, while causing a slight increase in the final pH of carbonation. This behavior is similar to that observed in atmospheric carbonation.

The formation of carbonate complexes of vanadate in high-pressure carbonation is also worth investigating. Figure 10 shows that the amounts of VO₂(CO₃)³⁻₂ and HVO₃CO₃²⁻ decrease slightly as the total pressure increases, and the former one is approximately 1.5 times more abundant than the latter one at 0.2–3.0 MPa. Furthermore, the amount of VO₂(CO₃)³⁻₂ is more sensitive to changes of carbonation temperature at 1 MPa, increasing from 0.054 mol/kg at 25 °C to 0.356 mol/kg at 55 °C, which may be due to the increased HCO₃⁻ concentration at higher temperatures.

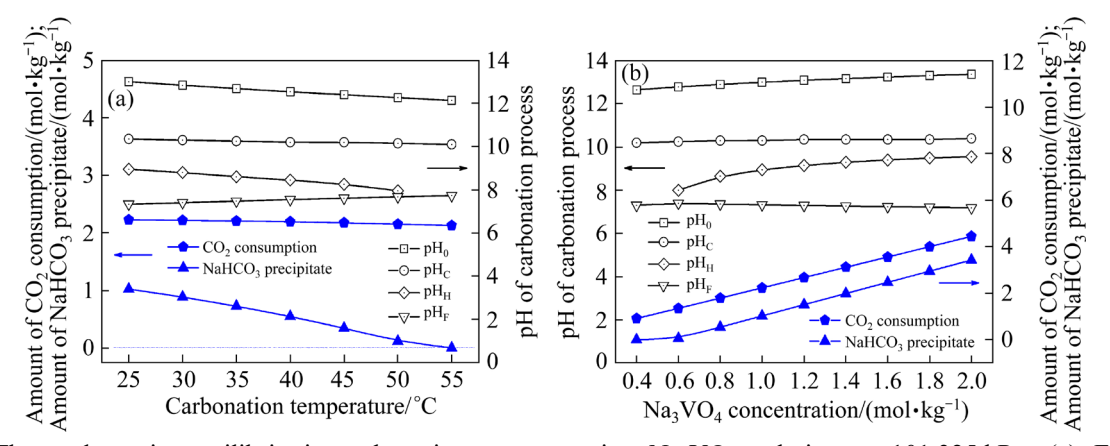


Fig. 8 Thermodynamic equilibria in carbonating representative Na_3VO_4 solution at 101.325 kPa: (a) Effect of carbonation temperature at [V]=1 mol/kg; (b) Effect of Na_3VO_4 concentration at 25 °C

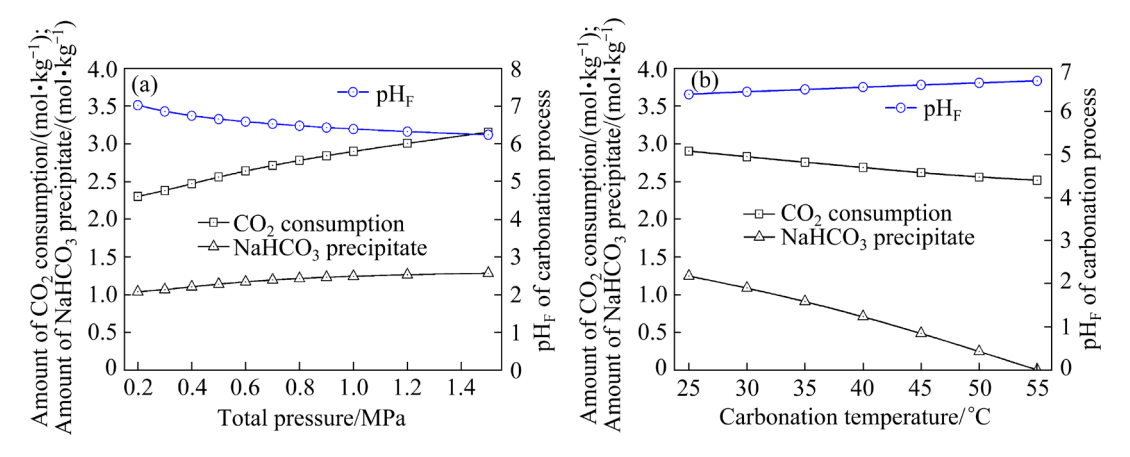


Fig. 9 Thermodynamic equilibria in carbonating representative Na_3VO_4 solution at high pressures: (a) Effect of total pressure at 25 °C; (b) Effect of carbonation temperature at 1 MPa

In high-pressure carbonation, gaseous CO₂ in the autoclave serves to maintain the gas-liquid equilibrium and is released into the air after a batch carbonation operation. The utilization efficiency of CO₂ can be calculated as the ratio of the C atoms in the aqueous solution to the total C atoms in the system, and Fig. 11 shows the calculation results under different total pressures and autoclave filling ratios (initial volume of the aqueous solution/total volume of the autoclave). When the autoclave filling ratio is 0.667, CO₂ utilization efficiency decreases almost linearly with increasing total pressure and remains at a high level of >85%. The CO₂ utilization efficiency at 1 MPa is significantly affected by the autoclave filling ratio, increasing from 77.0% at the filling ratio of 0.333 to 98.1% at the filling ratio of 0.833. The larger amount of gaseous CO2 at higher pressures and lower autoclave filling ratios can both lead to the low CO₂ utilization efficiency.

3.3.3 Vanadium precipitation and solution recycling To avoid introducing anionic impurities, (NH₄)₂CO₃ was selected to replace the commonly used (NH₄)₂SO₄ and NH₄Cl for precipitation. Na₃VO₄ solution without Si and Al impurities was used to simplify the calculations in this section. To determine the end point of carbonation before vanadium precipitation, it could be better to calculate and compare the thermodynamic equilibria by adding (NH₄)₂CO₃ into the carbonated solutions of Nos. A2 and A4 in Table 2. However, due to the lack of sufficient literature data [40,41] to regress the interactions of CO_3^{2-} - $H_2VO_4^-$ and HCO_3^- - $H_2VO_4^-$ pairs, the prediction of NH₄VO₃ solubility by OLI Studio software was unsatisfactory, and thus precipitation of NH₄VO₃ was not calculated. Fortunately, our experimental results show that after adding (NH₄)₂CO₃ into the solutions of Nos. A2 and A4 in Table 2 with the NH₄+/V molar ratio of 1:1,

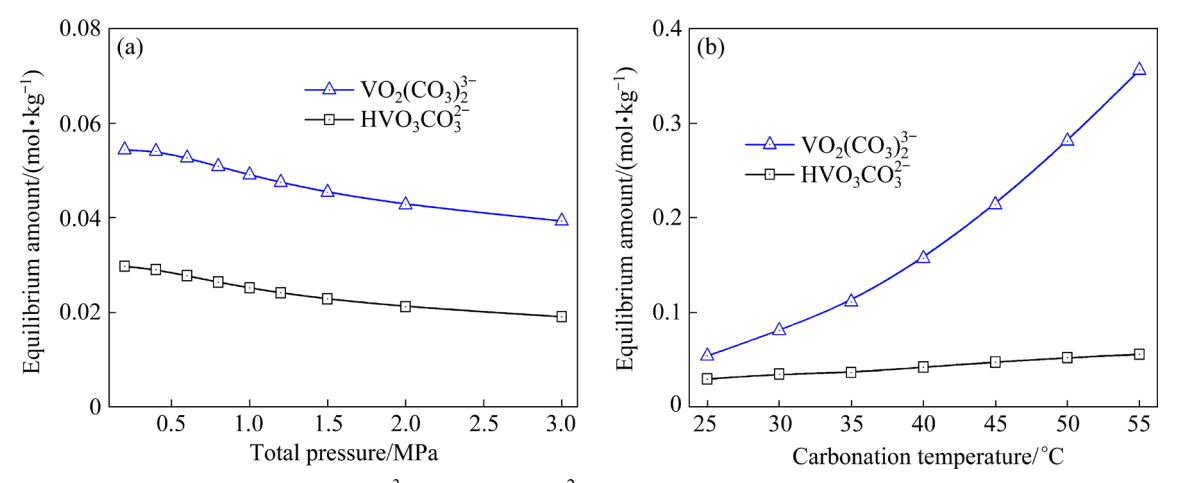


Fig. 10 Equilibrium amount of VO₂(CO₃)³⁻ and HVO₃CO₃²⁻ in carbonating representative Na₃VO₄ solution: (a) Effect of total pressure at 25 °C; (b) Effect of carbonation temperature at 1 MPa

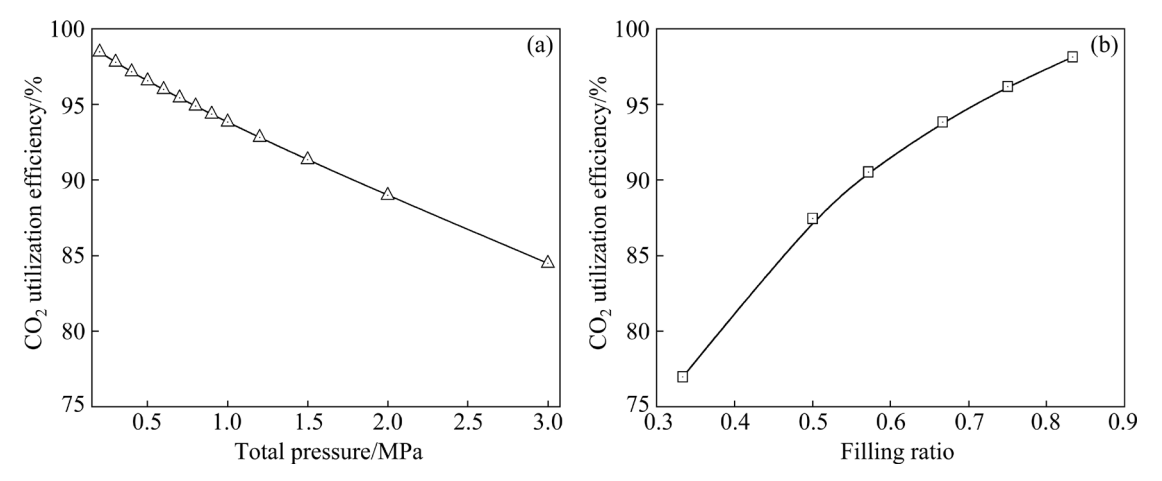


Fig. 11 Calculated CO₂ utilization efficiency at end of carbonating representative Na₃VO₄ solution at 25 °C: (a) Effect of total pressure at filling ratio of 0.667; (b) Effect of filling ratio at total pressure of 1 MPa

No.	Input/mol		Species output/mol				
			CO ₃ ²⁻	HCO ₃	NaHCO ₃ (s)	V-solid	
B1	$0.1 Na VO_3 + 0.05 (NH_4)_2 CO_3 + 1.45 Na_2 CO_3 + 55.5082 H_2 O$	10.34	1.341	0.145	0	0	
B2	$0.1 Na VO_3 + 0.05 (NH_4)_2 CO_3 + 1.1881 Na HCO_3 + 55.5082 H_2 O$	9.08	0.432	1.034	0.151	0	
В3	Aqueous {B1}+1.5136CO ₂	7.52	0.012	1.254	1.631	0	
B4	Aqueous $\{B3\}+0.9Na_3VO_4+1.4521H_2O$	10.07	1.179	0.190	0	0	
B5	Aqueous {B4}+0.3095CO ₂	9.40	0.935	0.720	0	0	

Table 3 Thermodynamic equilibria of vanadium precipitation, deep carbonation, and recycling remaining solution to dissolve solid Na₃VO₄ at 25 °C and 101.325 kPa

the vanadium precipitation efficiency was approximately 90% with NH₄VO₃ as the solid phase. Therefore, thermodynamic calculations were conducted using the composition of experimental solutions after vanadium precipitation, and the results are shown as Nos. B1 and B2 in Table 3.

Table 3 indicates that solid NaHCO₃ can precipitate from the solution of No. B2, which can lead to the contamination of NH₄VO₃ products and excessive sodium loss in vanadium precipitation. This indicates that the end point of the first carbonation of Na₃VO₄ solution before vanadium precipitation should be 9.3–9.4 (No. A2 in Table 2), at which Na₃VO₄ is basically transformed into Na₂CO₃ and NaVO₃.

The solution after vanadium precipitation contains a large amount of sodium (No. B1 in Table 3), which can be deeply carbonated with CO₂ to reach a pH of 7.5, resulting in 54.5% sodium precipitation from the solution (No. B3 in Table 3). Because of the low vanadium concentration in the solution after vanadium precipitation, NaHCO₃ precipitated from this solution cannot entrain too much vanadium, thus minimizing vanadium loss.

After deep carbonation, the solution still contains sodium, vanadium, and ammonia. Recycling the solution to dissolve solid Na_3VO_4 (No. B4 in Table 3) is a crucial step in the new process. At this stage, after mixing the recycled solution with solid Na_3VO_4 , the amount of CO_3^{2-} changes from 0.012 to 1.179 mol, and the main species of vanadium becomes $V_4O_{13}^{6-}$. The obvious transformation between vanadate and carbonate anions can be expressed as follows:

$$4VO_4^{3-}+6 HCO_3^{-}=V_4O_{13}^{6-}+6CO_3^{2-}+3H_2O$$
 (10)

Finally, the solution of B4 in Table 3 can be carbonated with $0.3095 \text{ mol } CO_2$ to reach a pH of

around 9.4 (No. B5 in Table 3), which can be used to precipitate vanadium in the next cycle.

3.4 Proposal of new process and experimental verification

According to the above thermodynamic calculations, a new process to stepwise precipitate NH₄VO₃ and NaHCO₃ from Na₃VO₄ solution based on regulating CO₂ carbonation was proposed, consisting of first carbonation, impurity removal, vanadium precipitation, deep carbonation, and solution recycling, as described in Fig. 12.

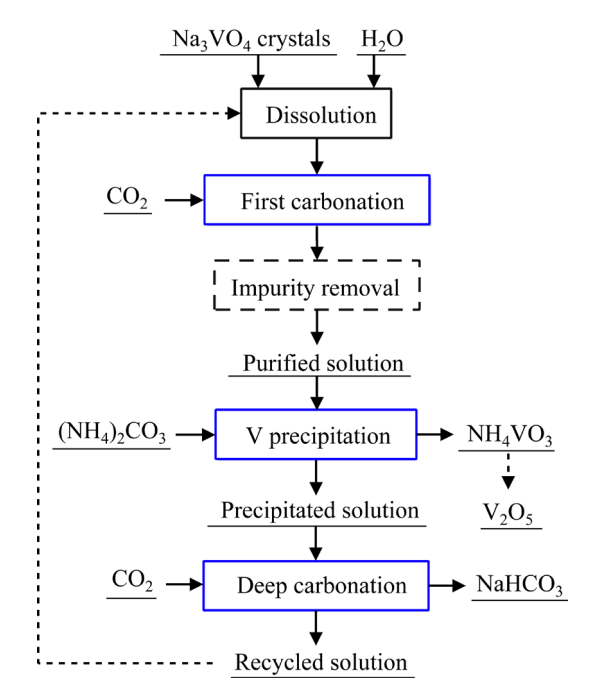


Fig. 12 Proposed flowsheet of new process for stepwise precipitation of NH₄VO₃ and NaHCO₃ using practical Na₃VO₄ crystals

The main steps in this new process are conducted at room temperature. During the first carbonation, atmospheric carbonation is employed to reach the solution pH of 9.3–9.4. After vanadium

precipitation by adding (NH₄)₂CO₃, high-pressure carbonation is preferred in deep carbonation, which can improve CO₂ utilization efficiency and reaction rate, and the final pH is 7.3–7.5. Most silicon impurities can be removed by adding NaAlO₂ after the first carbonation, and almost all aluminum can be removed due to the formation of dawsonite. The solution after vanadium precipitation and deep carbonation can be reused to dissolve solid Na₃VO₄ and repeat the above procedures, thus avoiding ammonia emission compared with the traditional process and ensuring higher recovery of vanadium and sodium. This study provides theoretical support for the green utilization strategy of high alkali solutions containing Na₃VO₄.

To verify the proposed process, the main steps were carried out with Na₃VO₄ solution containing 58.5 g/L V, 3.0 g/L Si, and 0.3 g/L Al, and repeated once with the recycled solution. Figure 13 presents the experimental concentrations of sodium and vanadium in different steps. Due to liquid entrainment in precipitates, the sodium loss after vanadium precipitation (P2) and vanadium loss after deep carbonation (D2) were 0.8% and 8.6%, respectively. By adding NaAlO2 into the first carbonated solution at 60 °C and subsequently washing the solid residue with water, 94% of the total silicon was removed, with a vanadium loss of only 0.11% per cycle. These indicate that 99.1% of vanadium and 91.4% of sodium in the input (S1) can be recovered in the form of NH₄VO₃ and NaHCO₃ in the subsequent steps, respectively, as

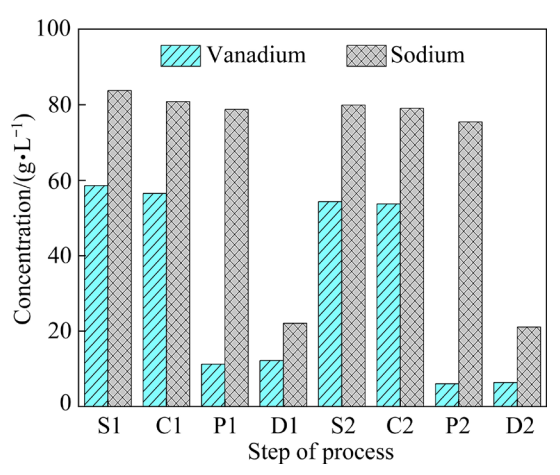


Fig. 13 Experimental concentrations of Na and V in different steps of new process (S–Dissolution, C–Carbonation, P–Vanadium precipitation, and D–Deep carbonation; numbers 1 and 2 represent the times of cycles)

confirmed by the XRD patterns shown in Fig. 14. Obtained NH_4VO_3 was purified by crystallization and calcinated at $550\,^{\circ}\text{C}$ for 2 h to prepare V_2O_5 , and the composition of V_2O_5 product was 99.51% V_2O_5 , 0.38% Na_2O , 0.06% SiO_2 , and 0.05% Al_2O_3 , which meets the requirement of 99.5% grade V_2O_5 powder in Chinese Standard YB/T 5034—2017.

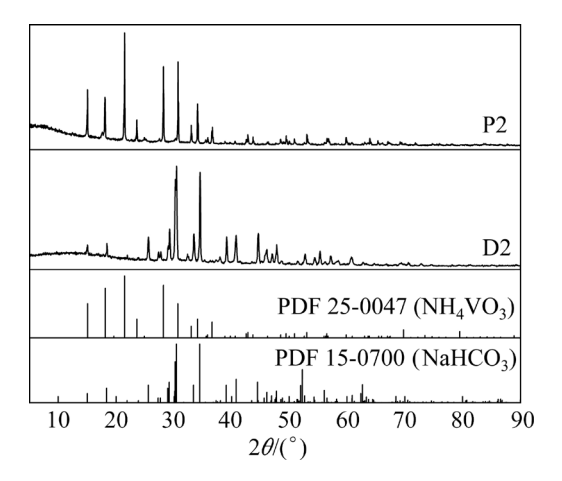


Fig. 14 XRD patterns of solids from vanadium precipitation (P2) and deep carbonation (D2)

4 Conclusions

- (1) A new V(V) speciation model for the aqueous solution containing vanadate and carbonate was established using credible thermodynamic data and the Bromley–Zemaitis activity model. The carbonation Na₃VO₄ solution with CO₂ can form NaVO₃, Na₂CO₃, and NaHCO₃.
- (2) Thermodynamic equilibrium calculations were performed to investigate the behavior of vanadium, carbon, and impurity species under different conditions. In atmospheric carbonation at 25 °C, vanadium distribution in $V_4O_{13}^{6-}$ and $V_4O_{12}^{4-}$ reaches 91.2% and 66.8% at pH of 9.3 and 7.3, respectively. In high-pressure carbonation at 25 °C, the concentrations of $VO_2(CO_3)_2^{3-}$ and $VO_3CO_3^{3-}$ remain relatively low, and VO_2 utilization efficiency is significantly affected by the autoclave filling ratio.
- (3) Based on thermodynamic simulations, a process for the stepwise precipitation of NH₄VO₃ and NaHCO₃ from Na₃VO₄ solution is proposed. Na₃VO₄ solution is initially carbonated to the pH of 9.3–9.4, followed by the precipitation of NH₄VO₃. The solution after vanadium precipitation is deeply carbonated to the final pH of 7.3–7.5 to recover

NaHCO₃. The remaining solution can recycle to dissolve Na₃VO₄ crystals, ensuring an efficient and green approach.

(4) The proposed process is well verified by experiments, showing that 99.0% of vanadium and 91.4% of sodium in Na₃VO₄ solution can be recovered, respectively.

CRediT authorship contribution statement

Fan-cheng MENG: Conceptualization, Methodology, Software, Formal analysis, Visualization, Writing – Original draft; Yong-chao WANG: Validation; Xin CHAI: Investigation; Ya-hui LIU: Writing – Review & editing; Li-na WANG: Supervision, Funding acquisition; De-sheng CHEN: Resources.

Declaration of competing interest

The authors declare that they have no known competing financial interests or personal relationships that could have appeared to influence the work reported in this paper.

Acknowledgments

The authors are grateful for the financial supports from the National Natural Science Foundation of China (No. 22078343), Strategic Priority Research Program of the Chinese Academy of Sciences (No. XDA0430103), and the National Key Research and Development Program of China (No. 2018YFC1900502).

Supplementary Materials

Supplementary Materials in this paper can be found at: http://tnmsc.csu.edu.cn/download/20-p3386-2023-0381-Supplementary_Materials.pdf.

References

- [1] WANG Shao-na, FENG Man, DU Hao, WEIGAND J J, ZHANG Yi, WANG Xin-dong. Determination of metastable zone width, induction time and primary nucleation kinetics for cooling crystallization of sodium orthovanadate from NaOH solution [J]. Journal of Crystal Growth, 2020, 545: 125721.
- [2] LI Lan-jie, GAO Xiao-yu, WANG Xin-dong, QI Jian, ZHAO Bei-bei, WAN He-li. A novel method to prepare high-purity V₂O₅ from Na₃VO₄ solution [J]. Journal of Materials Research and Technology, 2021, 15: 1678–1687.
- [3] YI Yi-Hui, SUN Hu, YOU Jin-xiang, ZHANG Jin, CAI Yuan, ZHANG Xin, LUO Jun, QIU Guan-zhou. Vanadium recovery from Na₂SO₄-added V-Ti magnetite concentrate via grate-kiln process [J]. Transactions of Nonferrous Metals Society of China, 2022, 32(6): 2019–2032.

- [4] VINCO J H, BOTELHO JUNIOR A B, DUARTE H A, ESPINOSA D C R, TENÓRIO J A S. Kinetic modeling of adsorption of vanadium and iron from acid solution through ion exchange resins [J]. Transactions of Nonferrous Metals Society of China, 2022, 32(7): 2438–2450.
- [5] ZHANG Yi-min, WANG Li-na, CHEN De-sheng, WANG Wei-jing, LIU Ya-hui, ZHAO Hong-xin, QI Tao. A method for recovery of iron, titanium, and vanadium from vanadium-bearing titanomagnetite [J]. International Journal of Minerals, Metallurgy, and Materials, 2018, 25(2): 131–144.
- [6] MENG Fan-cheng, CAO Lei, YANG Huan, LIU Ya-hui, WANG Li-na, CHEN De-sheng, ZHAO Hong-xin, ZHEN Yu-lan, WANG Meng, QI Tao. Determination and analysis of solubility of Na₃VO₄ in aqueous NaOH solutions containing Na₂CO₃, NaAlO₂, or Na₂SiO₃ at 298.15–353.15 K [J]. Journal of Chemical & Engineering Data, 2021, 66(4): 1574–1581.
- [7] WU Kang-hua, WANG Ya-ru, WANG Xin-ran, WANG Shao-na, LIU Biao, ZHANG Yi, DU Hao. Co-extraction of vanadium and chromium from high chromium containing vanadium slag by low-pressure liquid phase oxidation method [J]. Journal of Cleaner Production, 2018, 203: 873–884.
- [8] FENG Man, WANG Shao-na, DU Hao , ZHENG Shi-li, ZHANG Yi Solubility investigations in the NaOH–Na₃VO₄– Na₂CrO₄–Na₂CO₃–H₂O system at (40 and 80) °C [J]. Fluid Phase Equilibria, 2016, 409: 119–123.
- [9] QU Jin-wei., ZHANG Ting-an., NIU Li-ping., LV Guo-zhi., ZHANG Wei-guang. A novel technology to prepare sodium vanadate from V-Cr-bearing reducing slag [J]. Russian Journal of Non-Ferrous Metals, 2021, 62(1): 1-9.
- [10] ZHANG Xu-kun, MENG Fan-cheng, ZHU Zhao-wu, CHEN De-sheng, ZHAO Hong-xin, LIU Ya-hui, ZHEN Yu-lan, QI Tao, ZHENG Shi-li, WANG Meng. A novel process to prepare high-purity vanadyl sulfate electrolyte from leach liquor of sodium-roasted vanadium slag [J]. Hydrometallurgy, 2022, 208: 105805.
- [11] YING Zi-wen, HUO Man-xing, WU Gui-xuan, LI Jie, JU Yun, WEI Qi-feng, REN Xiu-lian. Recovery of vanadium and chromium from leaching solution of sodium roasting vanadium slag by stepwise separation using amide and EHEHPA [J]. Separation and Purification Technology, 2021, 269: 118741.
- [12] WANG Xue-wen, YANG Ming-e, MENG Yu-qi, GAO Da-xiong, WANG Ming-yu, FU Zi-bi. Cyclic metallurgical process for extracting V and Cr from vanadium slag: Part I. Separation and recovery of V from chromium-containing vanadate solution [J]. Transactions of Nonferrous Metals Society of China, 2021, 31(3): 807–816.
- [13] YANG Ming-e, YANG Hao-xiang, TIAN Sheng-hui, WANG Ming-yu, WANG Xue-wen. Cyclic metallurgical process for extracting V and Cr from vanadium slag: Part II. Separation and recovery of Cr from vanadium precipitated solution [J]. Transactions of Nonferrous Metals Society of China, 2021, 31(9): 2852–2860.
- [14] CHAI Xin, MENG Fan-Cheng, ZHANG Xiang-lan, ZHANG Xu-kun, SUN Lin-quan, WANG Li-na. Carbonation of Na₃VO₄ solution with CO₂ for recovery of NaHCO₃ and NH₄VO₃: Kinetic analysis of carbonation process [J]. Journal

- of Sustainable Metallurgy, 2023, 9(2): 588-598.
- [15] ZHOU Zu-de, LU Tao, LIAO De-yi, ZHANG Ze-tian. Extraction of V₂O₅ and recovery of sodium salt from natural soda roasted vanadium slag [J]. Iron Steel Vanadium Titanium, 1984, 9(1): 65-70. (in Chinese)
- [16] LONG Si-si, ZAHNG Guo-fan, FENG Qi-ming, OU Le-ming, LU Yi-ping. Desiliconisation of alkaline leaching solution of roasted stone coal with carbonation method [J]. Transactions of Nonferrous Metals Society of China, 2010, 20(Suppl.): 132–135.
- [17] WANG Qin-meng, GUO Xue-yi, TIAN Qing-hua, QU Sheng-li, Zhi WANG, HUANG Ming-xing. Thermodynamic modeling of antimony removal from complex resources in copper smelting process [J]. Transactions of Nonferrous Metals Society of China, 2022, 32(12): 4113–4128.
- [18] ZENG Li, WANG Man, XIAO Chao, WU Sheng-xi, ZHANG Gui-qing, GUAN Wen-juan, LI Qing-gang, CAO Zuo-ying. Enhancement of CaMoO₄ calcine decomposition and recovery of calcium resource by HCl cycle leaching [J]. Transactions of Nonferrous Metals Society of China, 2022, 32(4): 1314–1324.
- [19] PETTERSSON L, HEDMAN B, NENNER A M, INGEGÄRD A. Multicomponent polyanions. 36. Hydrolysis and redox equilibria of the H⁺-HVO₄²⁻ system in 0.6 M Na(Cl). A complementary potentiometric and 51V NMR study at low vanadium concentrations in acid solution [J]. Acta Chemica Scandinavica, Series A: Physical and Inorganic Chemistry, 1985, 39: 499-506.
- [20] SELLING A, ANDERSSON I, PETTERSSON L, SCHRAMM C. M, DOWNEY S L, GRATE J H. Multicomponent polyanions. 47. The aqueous vanadophosphate system [J]. Inorganic Chemistry, 1994, 33(14): 3141–3150.
- [21] ELVINGSON K, BARO A G, PETTERSSON L. Speciation in vanadium bioinorganic systems. 2. An NMR, ESR, and potentiometric study of the aqueous H⁺-vanadate-maltol system [J]. Inorganic Chemistry, 1996, 35(11): 3388-3393.
- [22] LARSON J W. Thermochemistry of vanadium (5+) in aqueous solutions [J]. Journal of Chemical and Engineering Data, 1995, 40(6): 1276–1280.
- [23] HU Bin, ZHANG Chang-da, DAI Yan-yang, WANG Xue-wen, WANG Ming-yu. Separation of vanadium and chromium in solution after vanadium precipitation by co-extraction with N263 and selective stripping with NaOH solution [J]. Hydrometallurgy, 2022, 208: 105798.
- [24] CRUYWAGEN J J. Protonation, oligomerization, and condensation reactions of vanadate(V), molybdate(VI), and tungstate(VI) [J]. Advances in Inorganic Chemistry, 2000, 49: 127–182.
- [25] GUSTAFSSON J P. Visual MINTEQ [EB/OL]. 2021–12–05. https://vminteq.com/.
- [26] PUIGDOMENECH I. Chemical Equilibrium Diagrams [EB/OL]. 2020–02–24. https://www.kth.se/che/medusa/.
- [27] MCCANN N, WAGNER M, HASSE H. A thermodynamic model for vanadate in aqueous solution–equilibria and reaction enthalpies [J]. Dalton Transactions, 2013, 42(7): 2622–2628
- [28] BARIN I. Thermochemical data of pure substances [M]. 3rd

- ed. Weinheim: VCH Verlag, 1997.
- [29] SHOCK E L, SASSANI D C, WILLIS M, SVERJENSKY D A. Inorganic species in geologic fluids: Correlations among standard molal thermodynamic properties of aqueous ions and hydroxide complexes [J]. Geochimica et Cosmochimica Acta, 1997, 61(5): 907–950.
- [30] MCCANN N, IMLE M, HASSE H. Carbonate complexes of vanadate [J]. Polyhedron, 2015, 95: 81–85.
- [31] ZHANG Wei-guang, ZHANG Ting-an, LV Guo-zhi, CAO Xue-jiao, ZHU Hang-yu. Thermodynamic study on the V(V)-P(V)-H₂O system in acidic leaching solution of vanadium-bearing converter slag [J]. Separation and Purification Technology, 2019, 218: 164-172.
- [32] LI Xiao-bin, SHEN Lei-ting, TONG Xiao-yi, QI Tian-gui, LIU Gui-hua, ZHOU Qiu-sheng, PENG Zhi-hong. Thermodynamic analysis on reaction behaviors of silicates in (NH₄)₂WO₄–(NH₄)₂CO₃–NH₃–H₂O system [J]. Transactions of Nonferrous Metals Society of China, 2018, 28(11): 2342–2350.
- [33] MOCK B, EVANS L B, CHEN C. Thermodynamic representation of phase equilibria of mixed-solvent electrolyte systems [J]. AIChE Journal, 1986, 32(10): 1655–1664.
- [34] BROMLEY L A. Thermodynamic properties of strong electrolytes in aqueous solutions [J]. AIChE Journal, 1973, 19(2): 313–320.
- [35] ZEMAITIS JUNIOR J F, Predicting vapor-liquid-solid equilibria in multicomponent aqueous solutions of electrolytes [M]//NEWMAN S A, BARNER H E, KLEIN M, SANDLER S I (Eds.) Thermodynamics of aqueous systems with industrial applications. Washington, DC: American Chemical Society, 1980: 227–246.
- [36] WANG Pei-ming, ANDERKO A, YOUNG R D. A speciation-based model for mixed-solvent electrolyte systems [J]. Fluid Phase Equilibria, 2002, 203(1/2): 141–176.
- [37] ZENG Yan, ZHANG Yan, LI Zhi-bao, DEMOPOULOS G P. Measurement and chemical modeling of the solubility of Na₂SiO₃·9H₂O and Na₂SiO₃ in concentrated NaOH solution from 288 to 353 K [J]. Industrial & Engineering Chemistry Research, 2014, 53(23): 9949–9958.
- [38] LUO Sui-ming. Determination of sodium hydroxide and sodium carbonate, or sodium carbonate and sodium bicarbonate in the vanadium-containing solution [J]. Chemical Metallurgy, 1983, 8(4): 152–153. (in Chinese)
- [39] MARINOS D, VAFEIAS M, SPARIS D, KOTSANIS D, BALOMENOS E, PANIAS D. Parameters affecting the precipitation of Al phases from aluminate solutions of the Pedersen process: The effect of carbonate content [J]. Journal of Sustainable Metallurgy, 2021, 7(3): 874–882.
- [40] TRYPUĆ M, KIEŁKOWSKA U. Solubility in the NH₄HCO₃ +NH₄VO₃+H₂O system [J]. Journal of Chemical & Engineering Data, 1996, 41(5): 1005–1007.
- [41] YANG Hong, DU Hao, WANG Shao-na, ZHENG Shi-li, ZHANG Yi. Solubility data in the ternary NH₄HCO₃– NH₄VO₃–H₂O and (NH₄)₂CO₃–NH₄VO₃–H₂O systems at (40 and 70) °C [J]. Journal of Chemical & Engineering Data, 2016, 61(7): 2346–2352.

碳酸化 Na₃VO₄ 溶液分步沉淀 NH₄VO₃ 和 NaHCO₃ 的热力学模拟

孟凡成 1,2, 王永超 1,2, 柴 鑫 1, 刘亚辉 1, 王丽娜 1,2, 陈德胜 1

1. 中国科学院 过程工程研究所 战略金属资源绿色循环利用国家工程研究中心,北京 100190; 2. 中国科学院大学 化学工程学院,北京 101408

摘 要:通过热力学模拟,设计了基于调节正钒酸钠溶液的碳酸化以分步沉淀偏钒酸铵和碳酸氢钠的新工艺。首先,利用 Bromley-Zemaitis 活度系数模型建立含钒酸盐和碳酸盐的水溶液中 V(V)的化学形态新模型。然后,进行常压或高压碳酸化过程的热力学平衡计算,以揭示钒、碳、钠和杂质的行为。为了保证钒产品的纯度和收率,正钒酸钠溶液先碳酸化至 pH 值为 9.3~9.4,然后加入碳酸铵得到偏钒酸铵沉淀。沉钒后溶液深度碳酸化至最终 pH 值为 7.3~7.5,以沉淀碳酸氢钠,剩余溶液返回用于溶解正钒酸钠晶体。最后,验证实验表明,溶液中 99.1%的钒和 91.4%的钠分别以偏钒酸铵和碳酸氢钠的形式得到回收。

关键词: 热力学; 正钒酸钠; 化学形态模型; 碳酸化; 沉钒; 碳酸氢钠

(Edited by Bing YANG)